

# The Color Constancy Problem: An Illumination Invariant Mapping Approach

Rafael Wiemker

Universität Hamburg, II. Institut für Experimentalphysik  
Mail: FB Informatik / KOGS, Vogt-Kölln-Str. 30, 22527 Hamburg, FRG  
<http://kogs-www.informatik.uni-hamburg.de/projects/censis/Fernerkundung>  
E-mail: [wiemker@informatik.uni-hamburg.de](mailto:wiemker@informatik.uni-hamburg.de)

**Abstract.** We suggest a novel approach to the Color Constancy Problem for multispectral imagery. Our approach is based on a dichromatic illumination model and filters out all spectral information which possibly stems from the illumination rather than from the reflectance of a given surface. Instead of recovering the reflectance signal, the suggested mapping produces a new only surface reflectance-dependent descriptor which is invariant against varying illumination. Sole input is the relative direct to diffuse illumination spectrum, no assumptions about the possible reflectance spectra are made.

The mapping is a purely pixel based, fast, one-pass matrix operation and can preprocess multispectral images in order to segment them into regions of homogeneous reflectance, unperturbed by varying illumination conditions.

## 1 Introduction

The Color Constancy Problem arises whenever one wants to distinguish and classify radiance spectra received by a multispectral sensor and does not have sufficient knowledge about the respective illuminating irradiances. The significant reflectance spectrum of a surface can only be retrieved from the measured radiance spectrum if the proper illuminating spectral irradiance is known.

There is no general solution to the Color Constancy Problem, but approaches with respect to various applications have been made [3][4][5][7]. Remotely sensed multispectral aerial imagery is sampled at typically 5 to 100 spectral bands (channels). We show that the abundance of spectral information allows to overcome the illumination uncertainty.

This paper starts off from a dichromatic illumination model, i.e., a direct and a diffuse irradiance spectrum, and Lambertian reflectance, while not making any assumptions about the reflectance spectra. We show how to retrieve the spectral reflectance information contained in the observed spectra which cannot possibly stem from varying illumination. We present a filter process which is purely pixel based and does not use context assumptions as e.g. supposedly homogeneous and continuous surface regions. Moreover it does not require multiple views of the same surfaces under different illuminations as in photometric stereo methods. In contrast to the well known homomorphic filtering [6] the here presented filtering takes place not in the *spatial* but rather in the *spectral* domain.

The suggested mapping can improve classification or segmentation of multispectral images. It is based on a physically meaningful and experimentally verified dichromatic illumination model.

## 2 Dichromatic Illumination

For multispectral remote sensing applications as well as for outdoor scenes in computer vision it is common to model the global illumination onto a horizontal surface  $\mathbf{E}_{\text{glob}} = \mathbf{E}_{\text{dir}} + \mathbf{E}_{\text{diff}}$  as a *dichromatic illumination* with two basic sources:

- *direct* illumination  $\mathbf{E}_{\text{dir}}$  (sunlight) from the sun approximated as a point source,
- *diffuse* illumination  $\mathbf{E}_{\text{diff}}$  (skylight) from the whole remaining upper hemisphere (distributed source).

The diffuse illumination  $\mathbf{E}_{\text{diff}}$  is generated by sunlight scattered on air molecules (Rayleigh-scatter) and aerosols (Mie-scatter). So direct and diffuse illumination have distinct spectra, the ratio of which can be well described [1][8] as:  $\mathbf{E}_{\text{diff}}/\mathbf{E}_{\text{glob}} \sim \lambda^{-a}$  with the wavelength  $\lambda$  in units of  $\mu\text{m}$ , and a typical exponent  $a = [1\dots4]$ .

For tilted surfaces the contributions of direct and diffuse illumination change with surface orientation. We find different angular dependencies for point and distributed sources respectively. As many small scale and man made objects are too small to be considered in a Digital Terrain Model (DTM), the surface orientation of a given surface patch often is not available. Consequently we cannot determine the mixture of the two illumination contributions to which a given surface patch is exposed. Also, for man made objects in aerial imagery we cannot assume smooth and continuous surfaces.

### 2.1 Illumination Dependent Spectral Variance

Depending on the sensor, we observe radiance spectra  $\mathbf{x} = (x_1, \dots, x_N)^T$  sampled at  $N$  spectral bands of wavelength  $\lambda_i$ . Assuming Lambertian reflection, the observed radiance spectra  $\mathbf{x}$  are given by the direct and diffuse illumination spectra  $\mathbf{n} = \mathbf{E}_{\text{dir}}$  and  $\mathbf{m} = \mathbf{E}_{\text{diff}}$  multiplied component-wise with the specific surface reflectance spectra  $\mathbf{r}$ :

$$x_i = r_i \mu (m_i + \eta n_i) \quad , \quad \mu, \eta > 0 \quad (1)$$

where  $\mu$  is an overall brightness factor, and  $\eta$  is the relative contribution of direct illumination. In order to separate illumination and reflectance we change into the logarithmic domain:

$$\ln x_i = \ln r_i + \ln \mu + \ln(m_i + \eta n_i) \quad . \quad (2)$$

Now we expand the illumination term into a Taylor series in  $\eta$  for  $\eta \approx 1$ :

$$\ln(x_i/r_i) = \ln \mu - \sum_{k=1}^{\infty} (-1)^k (k-1)! (\eta-1)^k \left( \frac{n_i}{n_i+m_i} \right)^k \quad (3)$$

$$\ln \mathbf{x} - \ln \mathbf{r} \approx c_0 \mathbf{1} + \sum_{k=1}^{K-1} c_k \hat{\mathbf{n}}^k = \mathbf{Q} \mathbf{c} \quad (4)$$

where  $\mathbf{c}$  is a coefficient vector, and the powers of  $\hat{\mathbf{n}}$  with  $\hat{n}_i = \frac{n_i}{n_i+m_i}$  form the columns of the  $N \times K$  matrix  $\mathbf{Q} = [\hat{\mathbf{n}}^0 \dots \hat{\mathbf{n}}^{K-1}]$ .

## 2.2 Experimental Results

We have recorded spectra ( $N = 1000$  spectral bands) of different surfaces including a Lambertian reference panel under arbitrary angles, illuminated by clear and hazy skies. A principal component analysis of the logarithm of the observed spectra for each surface shows that the variance is well described by two eigenvectors, which are *independent of the reflecting material*. The eigenvectors are in good agreement with the expected  $[\hat{\mathbf{n}}^0, \hat{\mathbf{n}}^1] \sim [\mathbf{1}, \lambda^{-a}]$  after ortho-normalization.

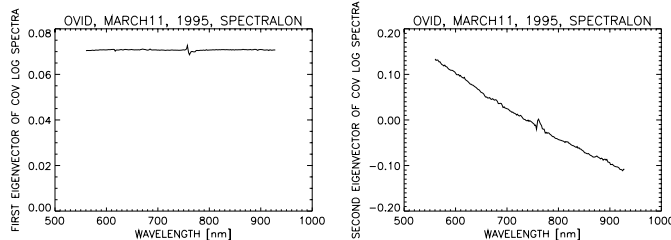


**Figure 1:** The two most significant eigenvectors of the covariance matrix of the logarithmic spectra observed under arbitrary angles.

## 3 The Filter Process

Now the aim is to filter out the variable components in order to produce an invariant spectral descriptor. The first  $K$  powers of  $\hat{\mathbf{n}}$  can be extracted from  $\ln \mathbf{x}$  by multiplication with the *orthogonal projector*  $\mathbf{P} = \mathbf{I} - \mathbf{Q}\mathbf{Q}^+$ , where  $\mathbf{Q}^+$  is the Moore-Penrose generalized inverse of  $\mathbf{Q}$ .

$$\ln \mathbf{x} \mapsto \ln \mathbf{x} - \mathbf{Q}\mathbf{Q}^+ \ln \mathbf{x} = \mathbf{P} \ln \mathbf{x} \quad (5)$$

$\mathbf{P} = \mathbf{P}^T$  is a symmetric  $N \times N$  matrix and has the defining projector property  $\mathbf{P}\mathbf{P} = \mathbf{P}$ ; it is thus an orthogonal projection  $\mathbb{R}^N \mapsto \mathbb{R}^{N-K}$ . Then the exponential function takes us back into the original domain:

$$\mathbf{x} \mapsto \exp(\mathbf{P} \ln \mathbf{x}) \quad (6)$$

The filtering process will necessarily remove reflectance information as well as illumination information. The basic idea is, however, that the reflectance spectra will differ in features which cannot possibly be explained by varying illumination. The experimental results (Fig. 1) show that the illumination covariance eigenvectors are smooth and of low frequency, and thus the filtering will not remove higher frequency reflectance features. As suggested by the experimental findings, we have achieved good results by filtering with a matrix  $\mathbf{Q}$  of rank  $K = 2$ .

## 4 Results on Simulated Data

In order to demonstrate the illumination invariance of the mapping, we have sampled four artificial spectral reflectance primitives at  $N = 40$  spectral bands (Fig. 2, left panel), and ‘exposed’ these reflectance spectra to various illuminations, i.e., multiplied them with different contributions  $\mu$  and  $\eta$  of typical direct

and diffuse illumination spectra (Eq. 1). Only for reasons of display they have been normalized to  $\mathbf{x}^T \mathbf{x} = 1$  in Figure 2 (center panel).

Then the discussed mapping (Eq. 6) has been applied to the simulated spectra, with  $K = 4$ . The mapped spectra (Fig. 2, right panel) show vanishing variance at different illuminations for a single reflectance spectrum, but the reflectance spectra 1 to 4 are still clearly distinguishable. In other words, if each spectral reflectance forms a spectral class, then the mapped spectra show vanishing in-class variance but remaining inter-class variance. Hence a subsequent classification process can assign the reflectance spectra to different spectral classes independently of their unknown respective illumination.

We have tested the robustness of the mapping by superposing strong random noise on our simulated data (signal to noise ratio  $\text{SNR} = 10$ ). In order to illustrate the effect which the mapping has in the spectral feature space, we have visualized the  $N = 40$  dimensional space by a principal components projection into a three dimensional subspace. Figure 3 (top row) shows that the simulated data of the four reflectance spectra is forming planes, which are contracted into points of vanishing in-cluster variance by the mapping. Figure 3 (bottom row) shows the same for the noisy data set, where the noise is propagated in a linear way.

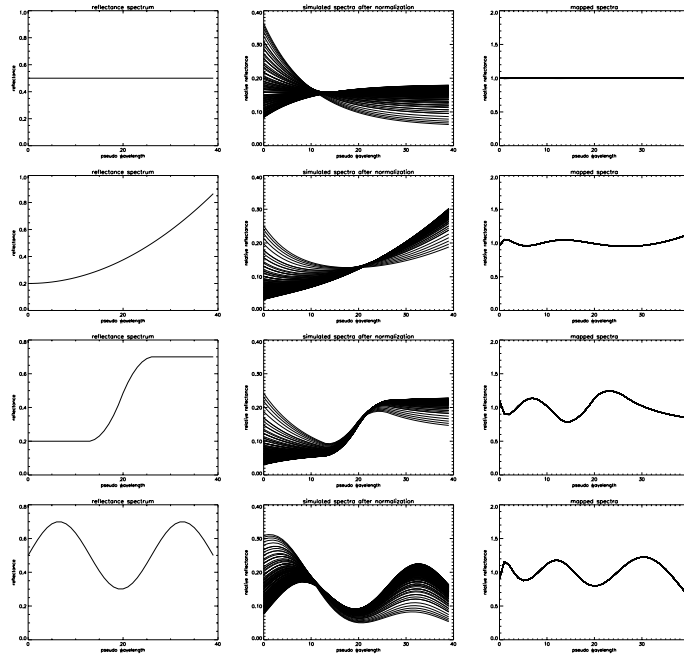


**Figure 2:** The artificial reflectance spectra 1 to 4 (left panel); the simulated noise-free ‘observed spectra’, i.e., the artificial reflectance spectra multiplied with various illumination spectra (center panel); and *all* these spectra after the mapping was applied (right panel).

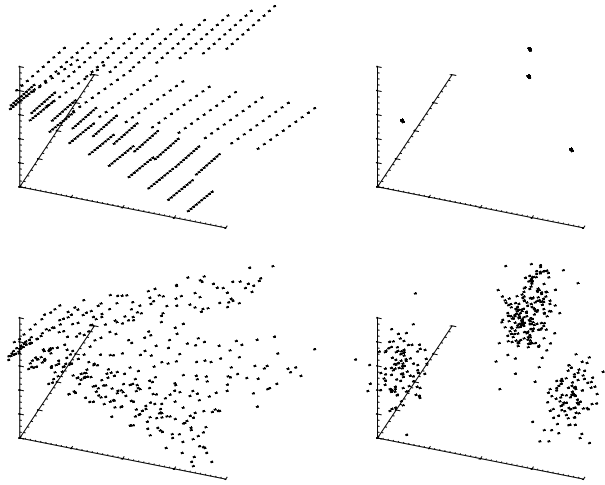


**Figure 3:** 3D projection of the spectral clusters in the feature space: the simulated data of all four reflectance spectra without noise (top left) forming four planes, the respective mapped spectra (top right) with vanishing in-cluster variance, the simulated data multiplied with noise SNR=10 (bottom left), the respective mapped spectra (bottom right).

The separability of two multivariate data clusters can be quantified by the Lawley-Hotelling trace criterion [2]. It describes the distance between the clusters in the multidimensional feature space relative to the expansion of their respective covariance ellipsoids:  $T^2 = \text{trace}(\mathbf{H} \mathbf{C}^{-1})$ , where  $\mathbf{H}$  is the inter-cluster covariance, and  $\mathbf{C}$  is the mean intra-cluster covariance matrix.

	$C_1$	$C_2$	$C_3$	$C_4$
$C_1$	0.0	$7.3 \cdot 10^4$	$7.2 \cdot 10^4$	$7.3 \cdot 10^4$
$C_2$		0.0	$7.2 \cdot 10^4$	$7.4 \cdot 10^4$
$C_3$			0.0	$7.4 \cdot 10^4$
$C_4$				0.0

	$C_1$	$C_2$	$C_3$	$C_4$
$C_1$	0.0	$1.2 \cdot 10^{12}$	$1.2 \cdot 10^{14}$	$2.0 \cdot 10^{14}$
$C_2$		0.0	$1.1 \cdot 10^{14}$	$2.2 \cdot 10^{14}$
$C_3$			0.0	$5.8 \cdot 10^{14}$
$C_4$				0.0

	$C_1$	$C_2$	$C_3$	$C_4$
$C_1$	0.0	$4.4 \cdot 10^4$	$5.1 \cdot 10^4$	$4.9 \cdot 10^4$
$C_2$		0.0	$4.6 \cdot 10^4$	$5.6 \cdot 10^4$
$C_3$			0.0	$5.8 \cdot 10^4$
$C_4$				0.0

	$C_1$	$C_2$	$C_3$	$C_4$
$C_1$	0.0	$1.9 \cdot 10^4$	$2.2 \cdot 10^5$	$1.9 \cdot 10^5$
$C_2$		0.0	$4.0 \cdot 10^5$	$2.7 \cdot 10^5$
$C_3$			0.0	$5.2 \cdot 10^5$
$C_4$				0.0

For the noisefree data before and after the mapping (Tables 1 and 2), the distances have increased almost infinitely as the clusters have essentially been contracted to a point which is the invariant signal. For the random noise data before and after the mapping (Table 3 and 4), the distances have still increased by one order of magnitude, except between reflectance spectra 1 and 2. For the last case we note that the low frequency differences in reflectance can indeed be mistaken for varying illumination and were removed as such.

## 5 Conclusion and Outlook

We have shown and experimentally verified that under dichromatic illumination the spectral variance of a surface observed under arbitrary angles is well described by two eigenvectors which are surface material independent. Filtering of these yields a spectral mapping which is invariant against varying illumination conditions. On simulated spectra we have shown the filtering to be robust against noise. Sole input is the relative direct illumination spectrum.

The aim of the discussed mapping is not to separate color and illumination signals; therefore the mapped spectra are not supposed to resemble the original reflectance spectra. The observed spectra are rather mapped to an *illumination invariant spectral descriptor*. The mapped spectra then allow to decide if observed spectra differ only because of varying illumination, or because of actual differences in reflectance.

Cluster analysis in the mapped feature space shows that the separability of different reflectances under varying illumination improves significantly. We can thus expect better performance of classification and segmentation.

We have recorded spectral data at outdoor experiments and thus verified the dichromatic illumination model. The next step will be the application of the suggested mapping to already recorded multispectral aerial imagery.

## Acknowledgement

This work was supported by the Volkswagen-Stiftung. I would like to thank Johann Bienlein, Leonie Dreschler-Fischer, Christian Drewniok, Martin Kollwe, Christoph Schnörr and Hartwig Spitzer for inspiring discussions, and Barbara Bartsch and Margareta Betancor for help with the OVID spectrometer.

## References

- [1] P. S. Chavez. Radiometric calibration of LANDSAT Thematic Mapper multispectral images. *Photogrammetric Engineering and Remote Sensing*, 55:1285–1294, 1989.
- [2] R. O. Duda and P. E. Hart. *Pattern Classification and Scene Analysis*. New York, 1973.
- [3] J. Ho, B. V. Funt, and M. S. Drew. Separating a color signal into illumination and surface reflectance components: Theory and applications. *IEEE Transactions on Pattern Analysis and Machine Intelligence*, 12(10):966–977, October 1990.
- [4] L. T. Maloney and B. A. Wandell. Color constancy: A method for recovering surface spectral reflectance. *J. Opt. Soc. Amer. A*, 3:29–33, 1986.
- [5] Y. Ohta and Y. Hayashi. Recovery of illuminant and surface colors from images based on the CIE daylight. In J.-O. Eklundh, editor, *Computer Vision - ECCV '94*, pages 235–246, Heidelberg, New York, 1994. Springer.
- [6] A. V. Oppenheim and R. W. Schaffer. *Digital Signal Processing*. London, 1975.
- [7] S. A. Shafer. Using color to separate reflection components. *COLOR Research and Application*, 10(4):210–218, 1985.
- [8] R. Wiemker and T. Hepp. Surface orientation invariant matching of spectral signatures. In *ISPRS Symposium on Spatial Information from Digital Photogrammetry and Computer Vision*, SPIE vol. 2357, pages 916–923, 1994.